Published OnlineFirst April 14, 2010; DOI: 10.1158/1078-0432.CCR-09-3066

Cancer Therapy: Preclinical

Clinical Cancer Research

Establishment and Characterization of a Panel of Human Uveal Melanoma Xenografts Derived from Primary and/or Metastatic Tumors

Fariba Némati[1], Xavier Sastre-Garau[2], Cécile Laurent[3,4,14], Jérôme Couturier[6], Pascale Mariani[7], Laurence Desjardins[8], Sophie Piperno-Neumann[9], Olivier Lantz[2], Bernard Asselain[3,4,10,14], Corine Plancher[10], Delphine Robert[2], Isabelle Péguillet[2], Marie-Hélène Donnadieu[2], Ahmed Dahmani[1], Marie-Andrée Bessard[1], David Gentien[11], Cécile Reyes[12], Simon Saule[5], Emmanuel Barillot[3,4,14], Sergio Roman-Roman[12], and Didier Decaudin[1,13]

Abstract

Purpose: Uveal melanoma is the most common primary intraocular malignant tumor in adults and is defined by a poor natural outcome, as 50% of patients die from metastases. The aim of this study was to develop and characterize a panel of human uveal melanoma xenografts transplanted into immunodeficient mice.

Experimental Design: Ninety tumor specimens were grafted into severe combined immunodeficient mice, and 25 transplantable xenografts were then established (28%). Relationship between tumor graft and clinical, biological, and therapeutic features of the patients included were investigated. Characterization of 16 xenografts included histology, molecular analyses by immunohistochemistry, genetic alteration analysis (single-nucleotide polymorphism), and specific tumor antigen expression by quantitative reverse transcription-PCR. Pharmacologic characterization (chemosensitivity) was also done in four models using two drugs, temozolomide and fotemustine, currently used in the clinical management of uveal melanoma.

Results: Take rate of human uveal melanoma was 28% (25 of 90). Tumor take was independent of size, histologic parameters, or chromosome 3 monosomy but was significantly higher in metastatic tumors. Interestingly, *in vivo* tumor growth was prognostic for a lower metastasis-free survival in patients with primary tumors. A high concordance between the patients' tumors and their corresponding xenografts was found for all parameters tested (histology, genetic profile, and tumor antigen expression). Finally, the four xenografts studied displayed different response profiles to chemotherapeutic agents.

Conclusions: Based on these results, this panel of 16 uveal melanoma xenografts represents a useful preclinical tool for both pharmacologic and biological assessments. *Clin Cancer Res; 16(8); 2352–62. ©2010 AACR.*

Uveal melanoma is the most common primary intraocular malignant tumor in adults. Despite the increased diagnostic accuracy and the development of conservative and effective treatments on primary tumor sites, such as plaque radiotherapy and photon beam therapy, the mortality remains stable and 50% of patients die from metastases that frequently involve the liver. Chemotherapy, such as oral temozolomide and intra-arterial fotemustine used at the metastatic stage, induces very low response rates, 14.3% and 36%, respectively, and a median survival time of 6.7 and 15 months (1–3). No postoperative adjuvant therapies are currently available to decrease the risk of metastases. Several prognostic factors of disseminated relapse after initial ophthalmologic treatment have been determined, including location with respect to the equator, monosomy 3, and retinal detachment (4). However, no effect of these prognostic markers on patient care can be envisaged in the absence of effective systemic therapies.

The growing body of knowledge about molecular and genetics events involved in oncogenesis and tumor progression has led to the identification of new therapeutic targets and therapeutic agents. Preclinical investigation in relevant models is therefore mandatory to select therapeutic agents before their assessment in clinical trials. To obtain preclinical results with high predictive value for

Authors' Affiliations: [1]Laboratory of Preclinical Investigation, Translational Research Department, Institut Curie; [2]Department of Tumor Biology, Institut Curie; [3]Institut Curie; [4]Institut National de la Sante et de la Recherche Medicale, U900; [5]Centre National de la Recherche Scientifique UMR146, Institut Curie; [6]Department of Genetics, Institut Curie; [7]Department of Visceral Surgery, Institut Curie; [8]Department of Ophthalmological Oncology, Institut Curie; [9]Department of Medical Oncology, Institut Curie; [10]Department of Statistics, Institut Curie; [11]Affymetrix Platform, Translational Research Department, Institut Curie; [12]Translational Research Department, Institut Curie; [13]Department of Clinical Hematology, Institut Curie, Paris, France and [14]Ecole des Mines de Paris, Fontainebleau, France

Note: Supplementary data for this article are available at Clinical Cancer Research Online (http://clincancerres.aacrjournals.org/).

Corresponding Author: Didier Decaudin, Laboratoire d'Investigation Pré-clinique/Service d'Hématologie Clinique, Institut Curie, 26 rue d'Ulm, 75.248 Paris cedex 05, France. Phone: 33-1-44-32-46-90; Fax: 33-1-53-10-40-11; E-mail: didier.decaudin@curie.net.

doi: 10.1158/1078-0432.CCR-09-3066

Published OnlineFirst April 14, 2010; DOI: 10.1158/1078-0432.CCR-09-3066

Translational Relevance

The prognosis of uveal melanoma patients remains generally poor, with a risk of metastatic relapse and relative inefficacy of conventional chemotherapies. New therapies, differing from classic treatments, are therefore warranted to improve the outcome of these patients. The treatment of cancer is continually improving due to growing knowledge of oncogenesis and the development of new targeted compounds. Early clinical trials evaluating such candidates require a large number of patients, are expensive, are time consuming, and expose patients to certain risks. *In vivo* preclinical assessment of antitumor agents in relevant animal models is a crucial step in the drug development process. We have therefore developed and characterized a panel of uveal melanoma xenografts obtained from human primary tumors to allow preclinical pharmacologic assessment and to explore the biology of this human cancer.

clinical trials, the choice of the tumor models on which new compounds and novel drug combinations are evaluated is critical. Human tumor fragments obtained from patients and directly transplanted into immunodeficient mice, known as primary xenografts or tumor grafts (5), are one category of recognized models used as tools for preclinical assays. Xenografts are known to reproduce the marked heterogeneity of human tumors and generally very closely resemble the patient's tumor in terms of histopathologic and molecular features, as well as response to therapy (6, 7). Furthermore, procedures for assessment of therapeutic efficacy are now well standardized and facilitate evaluation of combined therapies, particularly in terms of biostatistical analysis.

This study was designed to establish a panel of primary human uveal melanoma xenografts obtained from patient tumor samples transplanted into severe combined immunodeficient (SCID) mice. The resulting xenografts were then characterized and compared with the patient's original tumors, particularly in terms of molecular prognostic markers previously identified in human uveal melanomas and response to standard chemotherapies. Our data indicate that these models constitute a useful and relevant tool for preclinical assessment of new therapeutic approaches.

Materials and Methods

Patients and tumor samples. Ninety tumor specimens were obtained after enucleation of uveal melanoma, 73 from primary tumors (enucleation), and 17 from metastases. All patients had previously given their informed consent for experimental research on residual tumor tissue available after histopathologic and cytogenetic analyses. Some specimens were fixed in acetic acid, buffered formalin, alcohol solution (AFA) for further morphologic and immunohistochemical analysis, and others were stored in liquid nitrogen for further genomic analyses.

Data collection and statistical analysis. To define prognostic factors of *in vivo* tumor engraftment, the following patient characteristics were collected for the 90 cases included: gender, age, intraocular tumor location, thickness and diameter, retinal detachment, ciliary body and extrascleral tumor infiltration, primary treatment, histology, mitotic index, monosomy 3 (for available cases), primary tumor or metastatic sample, interval between diagnosis of primary tumor and first metastasis, and overall survival. A χ^2 test was used for univariate analysis. Survival curves were estimated using the Kaplan-Meier method (8). Statistical tests were two-sided and done using a 5% level of significance using the log-rank test. Metastasis-free survival was defined as the duration from initial diagnosis to first metastasis, and overall survival was measured from the date of initial diagnosis to the date of death irrespective of the cause.

Establishment of uveal melanoma xenografts. Fresh tumor samples obtained from pathologists were immediately transplanted into the interscapular fat pad of two to four non-preirradiated immunodeficient female SCID mice, 5 to 7 wk old, without any extracellular matrix preparation under total xylazine/ketamine anesthesia. Mice were maintained in a specific pathogen-free animal housing (Institut Curie) and regularly observed for tumor growth. Mice without growing tumors 1 y after initial transplantation were sacrificed. Animal care and housing were in accordance with the institutional guidelines of the French Ethics Committee (Ministère de l'Alimentation, de l'Agriculture et de la Pêche, Direction de la Santé et de la Protection Animale, Paris, France) and under the supervision of authorized investigators.

At a volume of ~1 cm^3, tumors were removed and subsequently transplanted to naive SCID mice. Samples were concomitantly stored frozen in DMSO-FCS solution or directly in liquid nitrogen and fixed in AFA for further studies. After three consecutive mouse-to-mouse passages, the xenograft was considered to be stabilized and was submitted to the process of standard characterization, including histopathologic, molecular, and genetic features, all of which were compared with the patient's tumor, and *in vivo* therapeutic assessments.

Histopathologic analyses. Morphologic examination was done on each xenograft and compared with the histologic findings of the corresponding patient's tumor. For light microscopy examination, 4-μm-thick AFA-fixed paraffin-embedded sections were stained with H&E safran. c-kit, Bcl-2, and β-catenin expressions were determined by immunohistochemistry. Antigen retrieval was done by incubating tissue sections for 20 min in 10 mmol/L citrate buffer (pH 6.1) in an 850 W microwave oven. Tissue sections were then incubated for 30 min with anti–c-kit (polyclonal rabbit, CD117; DAKO), anti–Bcl-2 (monoclonal mouse, clone 124; DAKO), or anti–β-catenin (monoclonal

Published OnlineFirst April 14, 2010; DOI: 10.1158/1078-0432.CCR-09-3066

mouse, 14/β-catenin; BD Biosciences) antibodies. Antibodies were diluted to 1:100 except for c-kit, which was diluted to 1:200. Staining was revealed by using the Vectastain Elite ABC peroxidase mouse IgG kit (Vector Laboratories) and diaminobenzidine (DAKO) as chromogen. Staining for the various tumor samples was assessed semiquantitatively. An isotypic control was done by using IgG1α FITC (1:1250 dilution; DAKO). Semiquantitative assessment was done by estimating at ×200 magnification, the percentage of positive neoplastic cytoplasms or nuclei defined within the area of highest positivity chosen after scanning the entire tumor surface at low power (10× objective).

Genomic analyses. To define the chromosome 3 copy number and loss of heterozygosity status and to detect other abnormalities, genetic analyses of the patients' tumors and the corresponding xenografts were done using Affymetrix Genome-Wide SNP Arrays 6.0. DNA was purified as described (9), and loss of heterozygosity of chromosome 3 was detected with single-nucleotide polymorphisms (SNP) as described (10). Data were analyzed using Partek Genomic Suite software, version 6.4, build 6.09.0129 (Partek, Inc.) using Partek's default parameters. Fluorescence *in situ* hybridization (FISH) and array comparative genomic hybridization (array-CGH) were done in two samples. FISH was done on intact nuclei after dissociation of the tumor fragment using a labeled centromeric probe specific for chromosome 3 (Vysis, Abbott Molecular) according to the supplier's protocol. For array-CGH, DNA extraction, labeling, and hybridization were done as previously described (11).

Expression of tumor-specific antigens. Expression of tumor-specific antigens was assessed by reverse transcription-PCR on RNA extracted from both frozen patient and tumor graft samples. Total RNA extraction was done by centrifugation on a CsCl cushion to totally eliminate melanin contamination. PCR amplification was carried out on cDNA (60 ng equivalent RNA) in the presence of 0.025 units/μL of Platinum Taq (Life Technologies), 200 μmol/L of deoxynucleotide triphosphate, and 0.4 μmol/L of each primer (12–14) in a final volume of 30 μL. After a denaturation cycle of 4 min at 94°C, amplification was run for 21 to 33 cycles (94°C for 1 min, annealing temperature of 1 to 2 min, 72°C for 1 min) according to Table 1 and followed by an extension cycle of 15 min at 72°C. Serial dilutions of 60 ng of equivalent RNA from melanoma cell lines were used for semiquantitative determination: SK23 for Melan-A, tyrosinase, and NA17; MZ2 cell line for MAGE1, MAGE2, MAGE3, MAGE6, and MAGE10; LB23 cell line for MAGE4; and LB373 cell line for LAGE1, LAGE2, and MAGE-C2. Annealing temperatures and amplification cycles were as follows: β-actin, 65°C for 1 min for 21 cycles; NA17, 62°C for 1 min for 33 cycles; tyrosinase, 65°C for 1 min for 25 cycles; Melan-A, 60°C for 1 min for 24 cycles; MAGE1, 72°C for 1 min for 31 cycles; MAGE2, 67°C for 1 min for 31 cycles; MAGE3, 72°C for 1 min for 31 cycles; MAGE4, 68°C for 1 min for 31 cycles; MAGE6, 70°C for 2 min for 31 cycles; MAGE10, 65°C for 1 min for 31 cycles; LAGE1, 62°C for 1 min for

Table 1. Clinical characteristics of all uveal melanoma patients (n = 90; univariate analysis) and *in vivo* tumor take rate (%)

Patients and tumor characteristics	Patients (n)	Tumor take rate (%)	P
Gender			
Male	47	23.4	NS
Female	43	32.6	
Age at diagnosis (y)			
<60	48	50.7	NS
≥60	42	49.2	
History of previous cancer			
No	86	25.6	NS
Yes	4	75.0	(0.06)
Primary tumor location			
Anterior to equator	3	0	
On equator	75	30.7	NS
Posterior to equator	11	18.2	
Origin of tumor sample			
Primary tumor	73	21.9	0.02
Metastatic tumor	17	52.9	
Primary tumor diameter (NA = 4)			
≤15 mm	18	16.7	NS
15-18 mm	27	37.0	
>18 mm	41	26.8	
Primary tumor thickness			
≤7 mm	17	29.4	NS
7-10 mm	14	42.8	
>10 mm	59	23.7	
Retinal detachment (NA = 2)			
No	31	38.7	NS
Yes	57	1.0	(0.07)
Extrascleral invasion (NA = 5)			
No	78	26.9	NS
Yes	7	28.6	
Primary tumor treatment			
No enucleation	17	35.3	NS
Enucleation	73	26.1	
Histology (n = 73)			
Epithelioid	29	31.0	
Spindle	19	36.8	NS
Mixed	23	13.0	
Ciliary body involvement (NA = 1)			
No	53	22.6	NS
Yes	19	36.8	
Extrascleral involvement (NA = 1)			
No	66	27.3	NS
Yes	6	16.7	
Mitotic index (NA = 9)			
Nil-low	72	24.2	NS
Medium-high	7	42.8	
Monosomy 3 of primary tumors (NA = 10)			
No	30	20.0	NS
Yes	33	33.3	
Initial treatment			
Proton therapy	73	35.3	NS
Enucleation	17	26.1	

Abbreviations: NA, not available; NS, not significant.

Published OnlineFirst April 14, 2010; DOI: 10.1158/1078-0432.CCR-09-3066

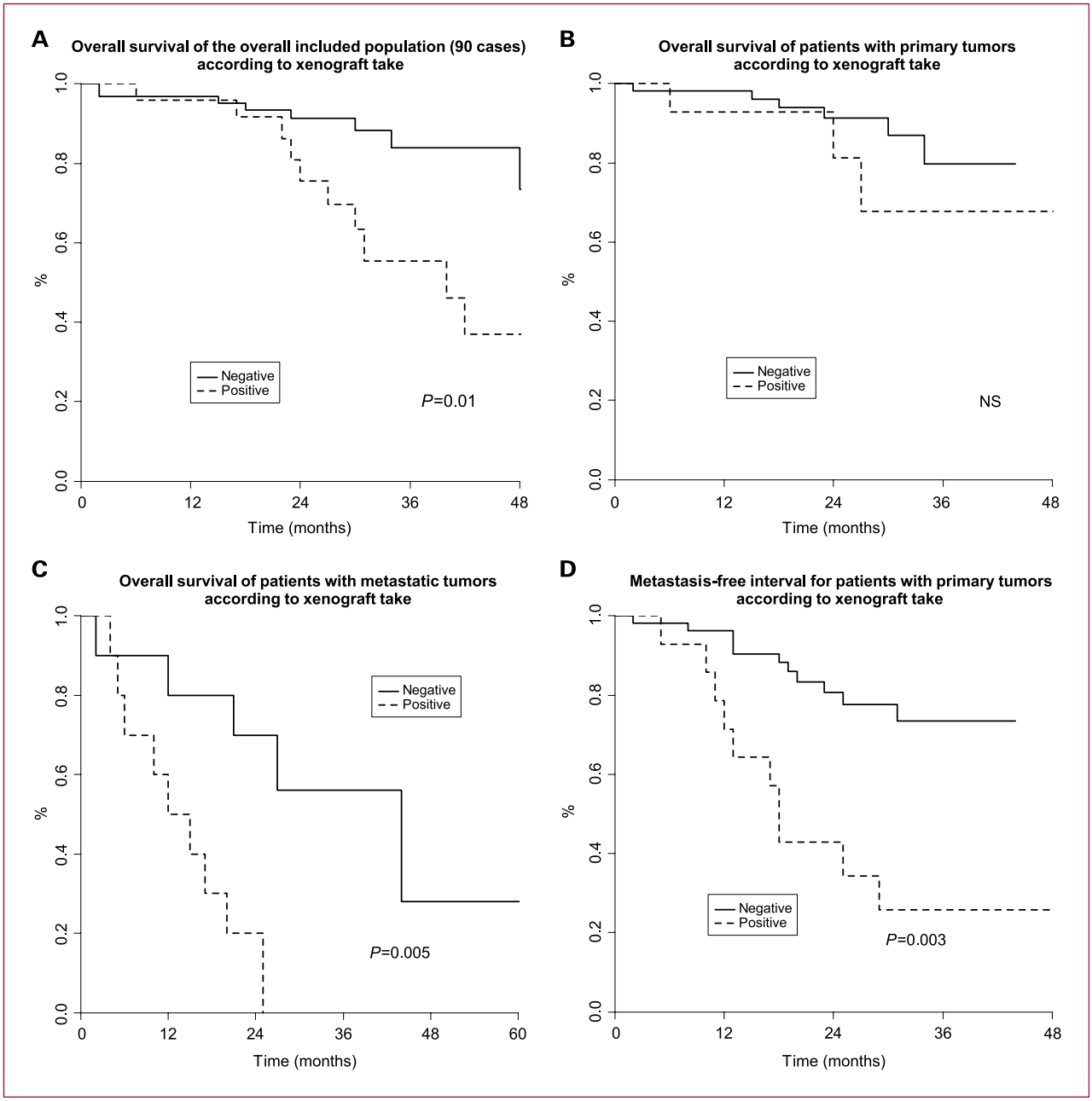

Fig. 1. Prognostic effect of *in vivo* tumor growth on survival of uveal melanoma patients. A, overall survival of the overall study population (90 cases) according to xenograft take. B, overall survival of patients with primary tumors according to xenograft take. C, overall survival of patients with metastatic tumors according to xenograft take. D, metastasis-free survival for patients with primary tumors according to xenograft take.

30 cycles; LAGE2, 62°C for 1 min for 30 cycles; and MAGE-C2, 60°C for 1 min for 30 cycles.

In vivo *tumor growth and antitumor efficacy of standard chemotherapeutic drugs.* For each new tumor graft model, *in vivo* spontaneous tumor growth was determined by the growth delay after transplantation, the time to reach a tumor volume of 40 to 200 mm^3, and the doubling time. For experimental therapeutic assays, female mice were xenografted with a tumor fragment of 15 mm^3. Mice bearing growing tumors with a volume of 40 to 200 mm^3 were individually identified and randomly assigned to the control or treatment groups (6-10 animals per group, as detailed in the tables and legends of the figures), and treatment was started on day 1. Animals with tumor volumes outside this range were excluded. Mice were weighed twice a week. Xenografted mice were sacrificed when their tumor reached a volume of 2,500 mm^3. Tumor volumes were calculated by measuring two perpendicular

Published OnlineFirst April 14, 2010; DOI: 10.1158/1078-0432.CCR-09-3066

diameters with calipers. Each tumor volume (V) was calculated according to the following formula: $V = a \times b^2 / 2$, where a and b are the largest and smallest perpendicular tumor diameters. Relative tumor volumes (RTV) were calculated from the following formula: RTV = (V_x/V_1), where V_x is the tumor volume on day x and V_1 is the tumor volume at initiation of therapy (day 1). Growth curves were obtained by plotting the mean values of RTV on the Y axis against time (X axis, expressed as days after start of treatment). Antitumor activity was evaluated according to tumor growth inhibition (TGI), calculated according to the following formula: percent GI = 100 − (RTVt / RTVc × 100), where RTVt is the median RTV of treated mice and RTVc is the median RTV of controls, both at a given time point when the antitumor effect was optimal. Fifty percent TGI was considered to be the limit for a meaningful biological effect. Statistical significance of differences observed between the individual RTVs corresponding to the treated mice and control groups was calculated by the two-tailed Student's t test. Growth delay index was calculated as the time required to reach the same RTV in the treated and control groups, at a RTV of 4.

Two cytotoxic drugs considered to be standard treatment for uveal melanomas were tested, namely, fotemustine (Muphoran, Servier) and temozolomide (Temodal, Schering Plough). Fotemustine was reconstituted in the appropriate solution according to the supplier, diluted in 5% dextrose, and administered i.p. at a dose of 30 mg/kg every 3 wk. Temozolomide was reconstituted in water and diluted in PBS/5% dextrose/Tween 80 (2/1/1‰) and administered orally in a 0.3 mL volume on day 1 every 4 wk. Mice were treated for three cycles.

Results

Establishment of xenografts. A total of 90 uveal melanoma samples obtained from primary tumors or metastases were implanted s.c. into SCID mice as described in Materials and Methods. Of the 90 tumors transplanted in immunodeficient mice, XX gave rise to viable tumors (take rate, 28%). Twenty-five of these tumors were shown to display uveal melanoma characteristics on histopathology. Molecular and genetic characterization was done on 16 models obtained from 10 primary ocular tumors (MP34/38/41/42/46/47/55/71/77/80), 5 liver metastases (MM26/28/52/66/74), and 1 skin metastasis (MM33). *In vivo* therapeutic evaluation was done on four models: MP77, MM66, MM26, and MP38.

Clinical characteristic of the 90 patients and their effect on the growth of the corresponding xenografted tumors are presented in Table 1. Briefly, gender, age, history of previous cancer, and tumor parameters such as tumor site,

Table 2. Histopathologic comparison between patient tumors and corresponding xenografts

Models	Histopathology		Chromosome 3		Bcl-2, % (intensity)*		c-kit, % (intensity)*		β-Catenin, % (intensity)*	
	P	X	P	X	P	X	P	X	P	X
MP34	E	E	—	L3p	70 (1)	0†	0	0	100 (3)	100 (3)
MP38	S	E	Isodisomy	L	80 (2)	80 (2)	60 (2)	50 (1)	100 (3)	100 (3)
MP41	E	E	N	N	90 (3)	90 (2)	0	0	100 (3)	70 (1)
MP42	S	S	N	N	‡	60 (1)	‡	0	‡	70 (2)
MP46	E	M	L (FISH)	Isodisomy	‡	‡	‡	‡	‡	‡
MP47	E	E	L	L (CGH)	80 (2)	90 (2)	10 (1)	10 (1)	100 (3)	90 (3)
MP55	M	E	L	L	100 (3)	100 (2)	15 (1)	0	60 (2)	100 (2)
MP71	E	E	Isodisomy	L	80 (2)	70 (2)	40 (1)	30 (2)	100 (3)	100 (3)
MP77	E	E	L	L	60 (1)	100 (2)	0	0	90 (2)	100 (3)
MP80	M	M	L	L	70 (1)	70 (2)	60 (2)	40 (2)	80 (2)	70 (2)
MM26	M	E	L	L	100 (2)	75 (2)	0	0	100 (2)	100 (3)
MM28	M	E	—	Isodisomy	100 (3)	100 (3)	20 (1)	60 (1)	100 (3)	100 (3)
MM33	E	E	N	N	100 (2)	80 (2)	0	10 (1)	90 (1)	100 (3)
MM52	M	M§	L	L	70 (2)	70 (1)	80 (2)	80 (2)	80 (2)	100 (3)
MM66	E	E	N	N	100 (2)	90 (2)	5 (1)	30 (1)	80 (2)	70 (2)
MM74	E	E	L	L	90 (2)	90 (2)	20 (1)	40 (1)	90 (3)	80 (3)

Abbreviations: MP, xenografts obtained from primary tumors; MM, xenografts obtained from metastases; P, patient's tumor; X, xenograft; E, epithelioid; S, spindle; M, mixed; N, normal; L, loss of heterozygosity.

*Data are expressed as % of positive tumor cells.

†Eighty percent necrosis in the tumor graft sample.

‡Major pigment overload prevented definition of the phenotype.

§Majority spindle.

Published OnlineFirst April 14, 2010; DOI: 10.1158/1078-0432.CCR-09-3066

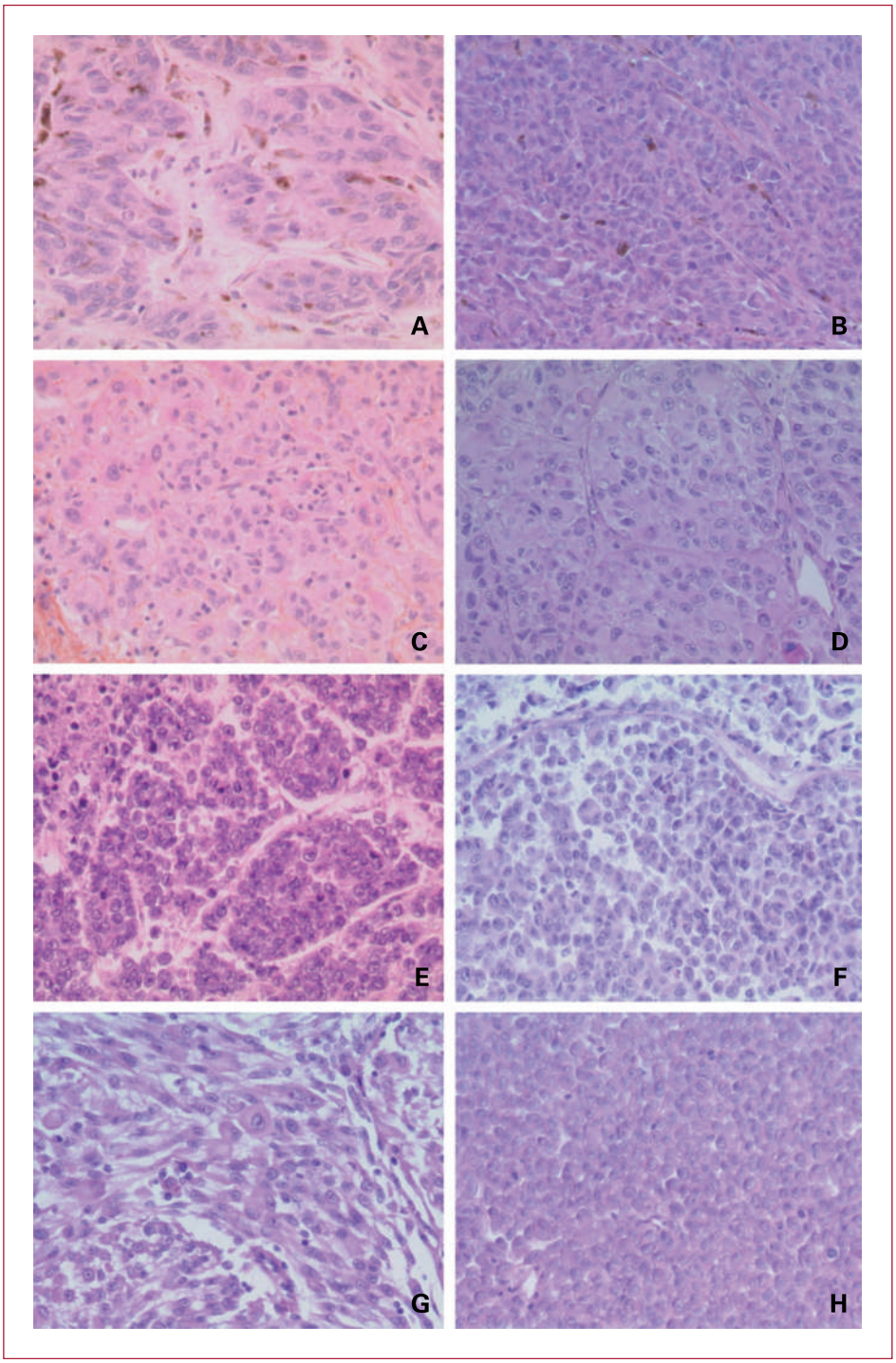

Fig. 2. Histopathologic features of four patient tumors and corresponding xenografts. MM26: patient (A) and xenograft (B); MM28: patient (C) and xenograft (D); MM66: patient (E) and xenograft (F); MP77: patient (G) and xenograft (H). H&E sections, ×200.

diameter and thickness, retinal detachment, and tumor externalization were not predictive of *in vivo* tumor take. Tumor growth was also independent of histologic parameters, such as epithelioid or spindle cell morphology, ciliary body involvement, mitotic index, and the presence of monosomy 3. Inversely, the tumor take rate was significantly increased when the tumor tissues were derived from metastases versus primary intraocular tumors, with take rates of 52.9% and 21.9%, respectively ($P = 0.02$). The 5-year overall survival of all patients included according to the *in vivo* tumor growth (growth/no growth) was 26% and 77%, respectively ($P = 0.01$; Fig. 1A). Tumor take in mice was predictive of a short overall survival in metastatic patients but not in primary tumor patients (Fig. 1B

Published OnlineFirst April 14, 2010; DOI: 10.1158/1078-0432.CCR-09-3066

and C). Interestingly, a significant correlation was shown between *in vivo* tumor growth and the 5-year metastasis-free survival of patients with a primary tumor (see Fig. 1D).

Histopathologic analyses. As shown in Table 2, the 16 uveal melanoma xenografts analyzed were composed of pure epithelioid cell in 9 cases, mixed with a predominance of epithelioid cells in 5 cases, and spindle cells in 1 case. In all but one case (MP38), histopathologic analyses showed a concordance between xenografts and the corresponding patient's tumor. For xenograft MP38, tumor cells were of the epithelioid type, whereas the patient had a spindle cell tumor. This apparent discrepancy could be explained by the presence of a small epithelioid contingent not observed on the histologic section. In three other cases of patient tumors with mixed cellularity, xenografts (MP55, MM26, and MM28) were defined as epithelioid cells, and in one case of a patient's epithelioid cell tumor, the corresponding xenograft (MP46) showed epithelioid cells, suggesting that these tumor cells may have a higher capacity for *in vivo* engraftment than spindle tumor cells. Four examples of patient tumors and corresponding xenografts are presented in Fig. 2.

To establish comparisons between xenografts and primary tumors, patient tumors, and their corresponding xenografts, the expression of three proteins was determined by immunohistochemistry for all patients and the corresponding xenografts (i.e., Bcl-2, c-kit, and β-catenin). The expression of these proteins was not affected by the localized or metastatic status of the tumors. Bcl-2 expression was similar in all 14 patient tumors and their corresponding xenografts, with a range of positive tumor cells from 60% (MP77) to 100% (MP55 and MM28) and an immunostaining intensity of 1 (14%), 2 (79%), and 3 (7%). A major pigment overload prevented Bcl-2 phenotyping in two cases. c-kit expression was heterogeneous and varied between 0% (four patients and their corresponding xenografts) and 80% (MM52) with a staining intensity of 1 (67%) and 2 (33%). Three xenograft and patient tumor couples presented slight variations in c-kit expression (MP55, MM33, and MM66). All 14 patient tumors and their corresponding xenografts presented a high level of β-catenin expression, between 70% and 100% of tumor cells, and a staining intensity of 1 (7%), 2 (27%), and 3 (66%), with complete concordance between tumor grafts and primary tumors in all cases.

Genomic analyses. To validate the concordance between patient tumors and the corresponding xenografts, genomic analyses focused on chromosome 3 status. As shown in Table 2, chromosome 3 status was determined by SNP array analyses in all 16 tumor grafts and in 14 corresponding patient tumors due to insufficient material in 2 cases. Moreover, except for patient tumor MP49 and xenograft MP47 analyzed by FISH and array-CGH, respectively, all analyses were done by SNP analysis. Of the 14 cases for which both xenograft and patient tumor were studied, 10 tumors presented loss of heterozygosity of chromosome 3 (either monosomy or isodisomy) and 4 had a normal chromosome 3 status. A good concordance was observed between patient tumors and their corresponding xenografts. The four tumors with disomic and heterozygous chromosome 3 led to xenografts with a similar chromosome 3 status. All chromosome 3 monosomic tumors led to monosomic xenografts. Interestingly, the two chromosome 3 isodisomic tumors led to monosomic xenografts. Minor differences in the genomic profiles of a tumor and its corresponding xenograft were also revealed by SNP arrays: in xenograft MP77 (derived from a chromosome 3 monosomic tumor), a homozygous loss was observed in 3p14.2 over ~250 kb (containing the *FHIT* gene, which shows aberrant transcripts in about one half of all esophageal, stomach, and colon carcinomas) and in 3q13.31 over 360 kb (containing a noncoding RNA). In xenograft MM26, a normal DNA copy number (two copies) was observed in 3p14.1 over 260 kb (containing the microphthalmia-associated transcription factor, which regulates differentiation of melanocytes in retinal pigment epithelium).

Expression of tumor-specific antigens. To compare xenografts and primary tumors, patient tumors and their corresponding xenografts were tested for 12 tumor-specific antigens (i.e., MAGE1, MAGE2, MAGE3, MAGE4, MAGE6, MAGE10, MAGE-C2, LAGE1, LAGE2, NA17, tyrosinase, and Melan-A). As shown in Supplementary Table S1, no MAGE and LAGE antigens were significantly expressed in either the patient tumors or their corresponding xenografts, except in two cases (patient tumor MP41 expressed LAGE2 <4% in comparison with 20-100% for the corresponding xenograft; patient tumor MP55 expressed MAGE1 to MAGE6 and no MAGE10, MAGE-C2, and LAGE1, whereas the corresponding xenograft expressed all MAGE and LAGE antigens except for MAGE-C2). Melan-A was expressed in all patient tumors and corresponding xenografts, with variations in the expression level in four cases (MP34, MP41, MP42, and MP46). NA17 was expressed in all cases. Finally, the level of expression of tyrosinase was similar between patient tumors and their corresponding xenografts, except in

Fig. 3. Effects of fotemustine and temozolomide in the four human uveal melanoma xenografts: MP77 (A and B), MM26 (C and D), MM66 (E and F), and MP38 (G and H). A, C, E, and G, fotemustine (●) was administered i.p. at a dose of 30 mg/kg every 3 wk. Mice in the control groups (○) received 0.2 mL of the drug-formulating vehicle with the same schedule as the treated animals. B, D, F, and H, temozolomide (■) was administered orally at a dose of 40 mg/kg day 1 to day 5 every 28 d. Mice in the control groups (□) received 0.3 mL of the drug-formulating vehicle with the same schedule as the treated animals. Treatments started when subcutaneous growing tumor volumes were 63 to 400 mm^3. Tumor growth was calculated by measuring two perpendicular diameters with calipers. Tumor volume and RTV were calculated as described in Materials and Methods. Growth curves were obtained by plotting mean RTV against time. Bars, SD. Fotemustine (n = 8-9 mice) and corresponding fotemustine control group (n = 8-10 mice); Temodal (n = 6-10 mice) and corresponding Temodal control group (n = 6-10 mice).

Published OnlineFirst April 14, 2010; DOI: 10.1158/1078-0432.CCR-09-3066

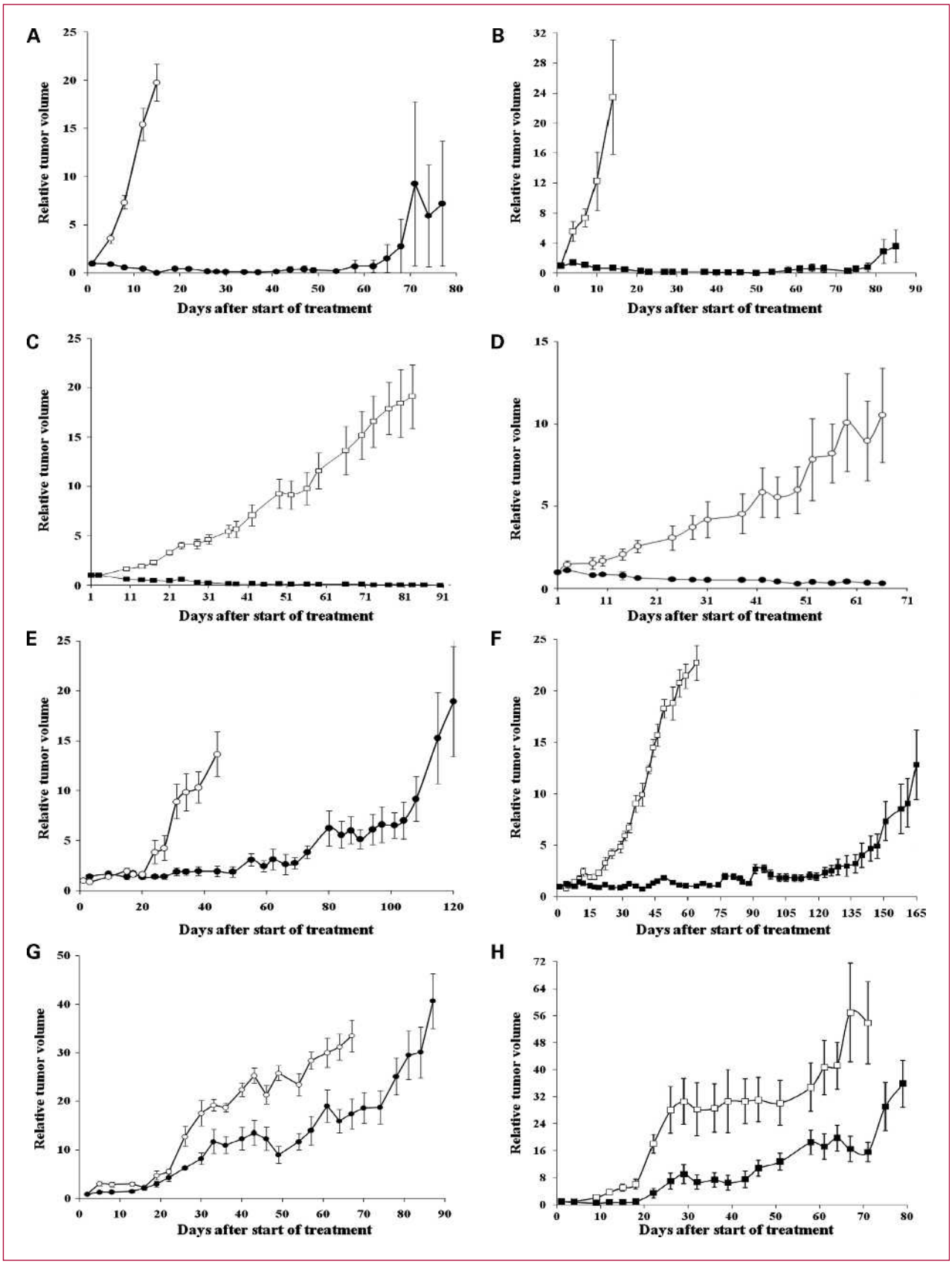

Published OnlineFirst April 14, 2010; DOI: 10.1158/1078-0432.CCR-09-3066

Table 3. *In vivo* efficacy of fotemustine and temozolomide in the four human melanoma xenografts tested

Models	Treatments	GDI (d)	TGI (%)	CR/total mice (%)	Median CR duration (d)
MP77	Fotemustine	13.8	100 (15)	8/9 (89)	58
	Temozolomide	21.3	97 (14)	7/8 (87)	36
MP38	Fotemustine	>3.75	100 (73)	7/9 (66)	(>48-30)
	Temozolomide	>2	97 (66)	0/9 (0)	—
MM26	Fotemustine	2.8	86 (44)	0/8 (0)	—
	Temozolomide	5.1	95 (59)	0/10 (0)	—
MM66	Fotemustine	1.2	65 (49)	0/8 (0)	—
	Temozolomide	1.8	86 (15)	2/6 (33)	5

Abbreviations: GDI, growth delay inhibition defined as the time required to reach the same RTV in the treated group and the control group (usually at a RTV of 4); CR, complete remission.

four cases (MP46, MP77, MM66, and MM74). A very marked difference was observed in one case (i.e., MM66) for which the patient's tumor did not express tyrosinase, whereas the xenograft expressed a level of 100%. However, it should be noted that for this tumor, derived from a liver metastasis, the patient's corresponding primary tumor expressed a high level of tyrosinase antigen (i.e., 100%), as in the metastasis-derived xenograft (data not shown).

In vivo ***tumor growth and antitumor efficacy of standard chemotherapeutic drugs.*** The characteristics of spontaneous tumor growth of the 16 characterized xenografts are shown in Supplementary Table S2. The main features were as follows: (*a*) the growth delay after initial transplantation ranged from 1 to 18 months; (*b*) after *in vivo* stabilization and serial transplantations, the time from transplantation to a tumor size of 60 to 200 mm^3 ranged from 20 days (MP77) to 132 days (MP38); and (*c*) the doubling time measured between 500 and 1,000 mm^3 ranged from 5 days (MP77) to 100 days (MP47).

Finally, to further characterize the established xenograft models, extensive therapeutic experiments with fotemustine and temozolomide, currently used in the treatment of metastatic uveal melanoma, were done. Four xenografts were chosen for pharmacologic characterization (Fig. 3; Table 3): xenograft MP77 obtained from a patient's primary tumor and displaying monosomy 3, xenograft MM26 obtained from a liver metastasis also displayed monosomy 3, xenograft MM66 obtained from a liver metastasis and defined by a disomy 3 status, and xenograft MP38 obtained from primary tumor with monosomy 3. *In vivo* responses to chemotherapy are shown in Fig. 3. For xenograft MP77, fotemustine and temozolomide were both cytotoxic, with optimal TGI of 100% and 97% and a growth delay index of 21.3 and 13.8 days, respectively (Fig. 3A and B). Both cytotoxic agents induced complete regression of the tumors in 89% and 87% of treated mice, respectively. However, in both situations, tumor relapse occurred after a median time of 58 days after fotemustine administration and 36 days after temozolomide treatment. Similarly, fotemustine and temozolomide were both highly effective on xenograft MP38, with an optimal GI of 100% and 97%, respectively (Fig. 3C and D). Optimal GIs induced by fotemustine and temozolomide on xenograft MM26 were 86% and 95%, respectively (Fig. 3E and F). Finally, no complete remission was observed after either treatment on xenograft MM66: fotemustine and temozolomide were less effective in this model, with an optimal GI of 65% and 86% and a growth delay index of 1.2 and 1.8, respectively (Fig. 3G and H). No complete remission was observed after either treatment.

Discussion

The aim of this study was to establish a panel of representative xenografts obtained from human uveal melanomas and to constitute a pharmacologic tool for drug efficacy evaluation. These tumor grafts were obtained by transplantation of human primary tumors or metastases into immunodeficient mice. Such validated tumor grafts could then be useful to test the antitumor efficacy of new agents or drug combinations to improve the clinical outcome of uveal melanoma patients. Various uveal melanoma models have been developed, mainly by inoculation into mice, rats, or rabbits of various established human cell lines obtained from primary or metastatic tumors, such as 92-1, SP-6.5, OCM-1, OCM-2, OCM-3, OCM-8, IPC227, OM431, C918, and M619 cells (15). Various injection modalities have also been used in orthotopic (16–18) and nonorthotopic situations (19). Similarly, a few genetic engineering models have been obtained by transforming uveal cells with oncogenic viruses (20). Primary tumor growth was observed in the retinal pigment epithelium and in metastatic lesions. One therapeutic experiment (dacarbazine and external beam irradiation) has already been reported (21). However, the prevalence of mice developing tumors remains low (i.e., ~20%) and insufficient for preclinical pharmacologic screening. Finally, two research teams have each developed a primary human tumor xenograft (16, 22). Establishment of a large panel

Published OnlineFirst April 14, 2010; DOI: 10.1158/1078-0432.CCR-09-3066

of uveal melanoma models therefore constitutes an essential step for preclinical experiments.

Ninety human uveal melanoma fresh tumors were grafted into SCID immunodeficient mice, and 25 tumor grafts were obtained (28%). Univariate analyses of prognostic factors for *in vivo* tumor growth showed that the origin of the patient's tumor samples was the only parameter significantly correlated with tumor take. Heegaard et al. (22) obtained only one tumor after eight grafts (13%). This tumor was histologically a mixed cell tumor, as was the patient tumor from whom the xenograft was established. The authors considered that the low tumor graft could be due to the stromal content of the tumor that might influence the take rate. The tumors investigated all had very scant stroma, which may have affected tumor nutrition immediately after transplantation and may have resulted in the low take rate.

In other human cancer types (i.e., breast cancers), pejorative clinical and biological factors are associated with an increased *in vivo* tumor take (6, 23, 24). As reported with other cancers (25), *in vivo* tumor growth in this study population constituted a predictive factor for overall survival and, in nonmetastatic patients, for metastasis-free survival. This observation could therefore be the basis for molecular studies in the two groups of tumors discriminated by their capacity to grow in immunodeficient mice.

Tumor graft characterization constitutes the first step of validation of the model and comprises histopathologic analyses done concomitantly in both tumor grafts and the corresponding patient tumors by a pathologist experienced in the field of human cancer. A very good concordance was observed between the histologic features of the patient's tumor and the corresponding xenografts. However, in a few cases of mixed or spindle cell uveal melanoma, an epithelioid uveal melanoma was diagnosed in the xenograft, suggesting that these tumor cells have a better capacity to survive and grow in mice, as reported by Liggett et al. (26). This observation is concordant with the fact that epithelioid uveal melanoma has a poorer prognosis than other forms (4, 27, 28). Immunohistochemical studies showed that xenografts preserved the characteristic properties of the patient's tumor. Bcl-2, previously shown to be highly expressed in uveal melanoma (29, 30), was expressed in all cases studied. The expression of c-kit, β-catenin, and tumor-specific antigens, studied in patient tumors and the corresponding tumor grafts, showed very few discordances, suggesting relative stability of tumor cell characteristics during the *in vivo* transplantation process. β-Catenin, described as a biomarker involved in class 2 tumor metastasis signature (27, 31, 32), was strongly expressed in all uveal melanoma samples and may explain the relatively high risk of metastatic disease for uveal melanoma patients.

Biological characterization of the models was completed by evaluating the response of four tumor grafts to conventional chemotherapy used in metastatic uveal melanoma patients (i.e., temozolomide and fotemustine). Three of the four models studied showed high sensitivity to treatment, with complete remissions but constant and rapid progression after stopping treatment. A similar situation was observed in uveal melanoma patients for whom the overall response rate after temozolomide and fotemustine administered in the metastatic setting was 14.3% and 36%, respectively, with a median response duration of 1.84 and 11 months (1–3, 33, 34). All these data therefore suggest that these uveal melanoma tumor grafts correlate with the clinical outcome of metastatic uveal melanoma patients and can be used for preclinical pharmacologic assessments. Moreover, the high complete remission rate in one model (MP77) is of particular interest to evaluate therapeutic compounds that could be concomitantly combined with chemotherapy or administered as adjuvant treatment, with a main readout defined as the relapse rate in both situations.

In conclusion, the present study describes a new panel of uveal melanoma tumor xenografts, corresponding to the clinical outcome observed in patients. Such a panel could therefore be useful for preclinical therapeutic experiments and for screening of new molecular markers of response and resistance. To improve the accuracy of our established models, as previously reported with other tumor cell lines (18, 35), we are currently developing orthotopic and/or liver metastatic tumors that might more closely mimic the natural characteristics and natural history of human uveal melanoma.

Disclosure of Potential Conflicts of Interest

No potential conflicts of interest were disclosed.

Acknowledgments

The costs of publication of this article were defrayed in part by the payment of page charges. This article must therefore be hereby marked *advertisement* in accordance with 18 U.S.C. Section 1734 solely to indicate this fact.

Received 11/19/2009; revised 01/15/2010; accepted 01/18/2010; published OnlineFirst 04/06/2010.

References

1. Peters S, Voelter V, Zografos L, et al. Intra-arterial hepatic fotemustine for the treatment of liver metastases from uveal melanoma: experience in 101 patients. Ann Oncol 2006;17:578–83.
2. Middleton MR, Grob JJ, Aaronson N, et al. Randomized phase III study of temozolomide versus dacarbazine in the treatment of patients with advanced metastatic malignant melanoma. J Clin Oncol 2000;18:158–66.
3. Bedikian AY, Papadopoulos N, Plager C, et al. Phase II evaluation of temozolomide in metastatic choroidal melanoma. Melanoma Res 2003;13:303–6.
4. Desjardins L, Levy-Gabriel C, Lumbroso-Lerouic L, et al. Prognostic factors for malignant uveal melanoma. Retrospective study on 2,241 patients and recent contribution of monosomy-3 research. J Fr Ophtalmol 2006;29:741–9.

Published OnlineFirst April 14, 2010; DOI: 10.1158/1078-0432.CCR-09-3066

5. Garber K. From human to mouse and back: 'tumorgraft' models surge in popularity. J Natl Cancer Inst 2009;101:6–8.
6. Marangoni E, Vincent-Salomon A, Auger N, et al. A new model of patient tumor-derived breast cancer xenografts for preclinical assays. Clin Cancer Res 2007;13:3989–98.
7. Arvelo F, Poupon MF, Goguel AF, et al. Response of a multidrug-resistant human small-cell lung cancer xenograft to chemotherapy. J Cancer Res Clin Oncol 1993;120:17–23.
8. Kaplan EL. Nonparametric estimation from incomplete observations. J Am Stat Assoc 1958;53:457–81.
9. Marty B, Maire V, Gravier E, et al. Frequent PTEN genomic alterations and activated phosphatidylinositol 3-kinase pathway in basal-like breast cancer cells. Breast Cancer Res 2008;10:R101.
10. Tuefferd M, De Bondt A, Van Den Wyngaert I, et al. Genome-wide copy number alterations detection in fresh frozen and matched FFPE samples using SNP 6.0 arrays. Genes Chromosomes Cancer 2008; 47:957–64.
11. Trolet J, Hupe P, Huon I, et al. Genomic profiling and identification of high-risk uveal melanoma by array CGH analysis of primary tumors and liver metastases. Invest Ophthalmol Vis Sci 2009;50:2572–80.
12. Chambost H, van Baren N, Brasseur F, Olive D. MAGE-A genes are not expressed in human leukemias. Leukemia 2001;15:1769–71.
13. Jacobs JF, Brasseur F, Hulsbergen-van de Kaa CA, et al. Cancer-germline gene expression in pediatric solid tumors using quantitative real-time PCR. Int J Cancer 2007;120:67–74.
14. Chambost H, Van Baren N, Brasseur F, et al. Expression of gene MAGE-A4 in Reed-Sternberg cells. Blood 2000;95:3530–3.
15. Beliveau A, Berube M, Carrier P, et al. Tumorigenicity of the mixed spindle-epithelioid SP6.5 and epithelioid TP17 uveal melanoma cell lines is differentially related to α5β1 integrin expression. Invest Ophthalmol Vis Sci 2001;42:3058–65.
16. Cheng H, Wu ZY, Zheng JL, et al. A preliminary study in establishment of mice model of experimental uveal melanoma. Zhonghua Yan Ke Za Zhi 2006;42:733–7.
17. Braun RD, Vistisen KS. Measurement of human choroidal melanoma xenograft volume in rats using high-frequency ultrasound. Invest Ophthalmol Vis Sci 2008;49:16–22.
18. Wang S, Coleman EJ, Pop LM, et al. Effect of an anti-CD54 (ICAM-1) monoclonal antibody (UV3) on the growth of human uveal melanoma cells transplanted heterotopically and orthotopically in SCID mice. Int J Cancer 2006;118:932–41.
19. Verin P, Meunier J, Gendre P, et al. Graft of a uveal melanoma on hamster kidney; ultrastructure of the original tissue and of cultivated fragments. Bull Soc Ophtalmol Fr 1971;71:170–4.
20. Albert DM, Shadduck JA, Liu HS, et al. Animal models for the study of uveal melanoma. Int Ophthalmol Clin 1980;20:143–60.
21. Syed NA, Windle JJ, Darjatmoko SR, et al. Transgenic mice with pigmented intraocular tumors: tissue of origin and treatment. Invest Ophthalmol Vis Sci 1998;39:2800–5.
22. Heegaard S, Spang-Thomsen M, Prause JU. Establishment and characterization of human uveal malignant melanoma xenografts in nude mice. Melanoma Res 2003;13:247–51.
23. Sharkey FE, Fogh J. Considerations in the use of nude mice for cancer research. Cancer Metastasis Rev 1984;3:341–60.
24. Fogh J, Orfeo T, Tiso J, Sharkey FE. Establishment of human colon carcinoma lines in nude mice. Exp Cell Biol 1979;47:136–44.
25. John T, Li M, Panchal D, et al. Correlation of primary tumor engraftment in immune deficient mice and relapse rate in patients with early-stage non-small cell lung carcinoma (NSCLC) [abstract 11082]. J Clin Oncol 2009;27.
26. Liggett PE, Lo G, Pince KJ, et al. Heterotransplantation of human uveal melanoma. Graefes Arch Clin Exp Ophthalmol 1993;231: 15–20.
27. Chang SH, Worley LA, Onken MD, Harbour JW. Prognostic biomarkers in uveal melanoma: evidence for a stem cell-like phenotype associated with metastasis. Melanoma Res 2008;18:191–200.
28. Damato B. Developments in the management of uveal melanoma. Clin Experiment Ophthalmol 2004;32:639–47.
29. Triozzi PL, Eng C, Singh AD. Targeted therapy for uveal melanoma. Cancer Treat Rev 2008;34:247–58.
30. Sulkowska M, Famulski W, Bakunowicz-Lazarczyk A, et al. Bcl-2 expression in primary uveal melanoma. Tumori 2001;87:54–7.
31. Zuidervaart W, Pavey S, van Nieuwpoort FA, et al. Expression of Wnt5a and its downstream effector β-catenin in uveal melanoma. Melanoma Res 2007;17:380–6.
32. Conway RM, Cursiefen C, Behrens J, et al. Biomolecular markers of malignancy in human uveal melanoma: the role of the cadherin-catenin complex and gene expression profiling. Ophthalmologica 2003;217:68–75.
33. Voelter V, Diserens AC, Moulin A, et al. Infrequent promoter methylation of the MGMT gene in liver metastases from uveal melanoma. Int J Cancer 2008;123:1215–8.
34. Leyvraz S, Spataro V, Bauer J, et al. Treatment of ocular melanoma metastatic to the liver by hepatic arterial chemotherapy. J Clin Oncol 1997;15:2589–95.
35. Yang H, Fang G, Huang X, et al. *In-vivo* xenograft murine human uveal melanoma model develops hepatic micrometastases. Melanoma Res 2008;18:95–103.

Clinical Cancer Research

Correction: Establishment and Characterization of a Panel of Human Uveal Melanoma Xenografts Derived from Primary and/or Metastatic Tumors

In this article (Clin Cancer Res 2010;16:2352–62), which was published in the April 15, 2010, issue of *Clinical Cancer Research* (1), there was an error in the legend of Fig. 3. The corrected legend appears below.

Fig. 3. Effects of fotemustine and temozolomide in the four human uveal melanoma xenografts: MP77 (A and B), MP38 (C and D), MM26 (E and F), and MM66 (G and H). A, C, E, and G, fotemustine (●) was administered i.p. at a dose of 30 mg/kg every 3 wk. Mice in the control groups (○) received 0.2 mL of the drug-formulating vehicle with the same schedule as the treated animals. B, D, F, and H, temozolomide (■) was administered orally at a dose of 40 mg/kg day 1 to day 5 every 28 d. Mice in the control groups (□) received 0.3 mL of the drug-formulating vehicle with the same schedule as the treated animals. Treatments started when subcutaneous growing tumor volumes were 63 to 400 mm3. Tumor growth was calculated by measuring two perpendicular diameters with calipers. Tumor volume and RTV were calculated as described in Materials and Methods. Growth curves were obtained by plotting mean RTV against time. Bars, SD. Fotemustine (n = 8-9 mice) and corresponding fotemustine control group (n = 8-10 mice); Temodal (n = 6-10 mice) and corresponding Temodal control group (n = 6-10 mice).

Reference

1. Némati F, Sastre-Garau X, Laurent C, Couturier J, Mariani P, Desjardins L, Piperno-Neumann S, Lantz O, Asselain B, Plancher C, Robert D, Péguillet I, Donnadieu MH, Dahmani A, Bessard MA, Gentien D, Reyes C, Saule S, Barillot E, Roman-Roman S, Decaudin D. Establishment and characterization of a panel of human uveal melanoma xenografts derived from primary and/or metastatic tumors. Clin Cancer Res 2010;16:2352–62.

Published OnlineFirst 07/13/2010.

doi: 10.1158/1078-0432.CCR-10-1531

Published OnlineFirst April 14, 2010; DOI: 10.1158/1078-0432.CCR-09-3066

Clinical Cancer Research

Establishment and Characterization of a Panel of Human Uveal Melanoma Xenografts Derived from Primary and/or Metastatic Tumors

Fariba Némati, Xavier Sastre-Garau, Cécile Laurent, et al.

Clin Cancer Res 2010;16:2352-2362. Published OnlineFirst April 14, 2010.